MDPI

Article

Complex Oxide Nanoparticle Synthesis: Where to Begin to Do It Right?

Elizabeth Gager [1,*] , William Halbert [2] and Juan C. Nino [1]

1 Department of Materials Science and Engineering, University of Florida, Gainesville, FL 32611, USA
2 Department of Chemical Engineering, University of Florida, Gainesville, FL 32611, USA
* Correspondence: egager@ufl.edu

Abstract: Synthesis of advanced ceramics requires a high degree of control over the particle size and stoichiometry of the material. When choosing a synthesis method for complex oxides it is important to begin with the correct precursors and solvents to achieve high purity nanoparticles. Here, we detail the selection process for precursors and solvents for liquid-phase precipitation synthesis. Data for metal nitrate, chloride, acetate, and oxalate precursors has been compiled to assist future synthesis. The role of hydration within the precursors is discussed as it affects the final stoichiometry of the material. Melting temperatures are also compiled for these compounds to assist in material selection. The solubility of the precursors in different solvents is examined to determine the correct solvent during synthesis. As an example, using the methodology presented here, two different materials are synthesized based on commonly available precursors. A catalyst based on a quaternary perovskite and an advanced ionic conductor based on a high entropy fluorite oxide are synthesized using precipitation methods and their characterization is detailed.

Keywords: co-precipitation; complex oxides; multicomponent oxides

1. Introduction

Traditional ceramics have been used for centuries dating back to when clays were molded and baked to be used as cooking utensils and storage containers [1]. The complexity of ceramics has since increased with the modern use of advanced ceramics over the last 100 years. As an early use of advanced ceramics, spark plugs turned to high purity alumina when porcelain proved to be insufficient for use, requiring new synthesis methods [2]. Since this, the range of advanced ceramics has expanded to many different areas including structural, electrical, and optical applications. The use of advanced ceramics allows for tailoring of the composition to improve the performance of the material. Multicomponent oxides are of particular interest with multiple dopants at varying levels of concentration to adjust the performance of the sample to meet various specifications.

To synthesize ceramics, two generalized approaches can be used: top-down synthesis and bottom-up synthesis. Top-down synthesis works to break down a bulk material into smaller components. A common method is ball milling to break down a material to smaller particle size for use. Top-down synthesis is generally limited to large particle size, unable to achieve homogenous nanosized particles. Therefore, to achieve nanosized particles for better performing materials, the need to produce ceramics in a variety of ways developed. Bottom-up synthesis techniques, shown in Figure 1, build from the atomic level using individual atoms or their clusters as building blocks. This allows for atomic mixing to produce homogeneous finely dispersed nano-sized particles. The methods used for multicomponent (i.e., ternary, quaternary, etc.) oxides can be broken down into three categories: solid-phase synthesis, liquid-phase synthesis, and vapor-phase synthesis.

Bottom-Up Synthesis

Solid-phase synthesis

Solid-solid
Solid-vapor

Disadvantages

Large final particle size
Reduced purity from
grinding

Advantages

Requires little equipment

Liquid-phase synthesis

Precipitation
Hydrolysis
Solvent evaporation
Citrate gel

Disadvantages

Small batch size

Advantages

Requires little equipment
Small particle size
High purity

Vapor-phase synthesis

Chemical vapor deposition
Physical vapor deposition

Disadvantages

Expensive equipment
Films, whiskers, bulk
crystals

Advantages

High purity

Figure 1. Examples of the three types of synthesis methods (solid-phase, liquid-phase, and vapor-phase) and the pros and cons of each used in bottom-up synthesis. Due to issues with solid-phase and vapor-phase synthesis methods, liquid-phase synthesis is generally the desired synthesis method for high purity nanoparticles.

Solid-phase synthesis is a simple method generally starting with oxides, carbonates, or hydroxides to decompose into the desired phase or chemically react with another material to form a new composition. While useful for some complex oxides, it is limited in use due to large particle size resulting from high temperature. Mechanical milling can be introduced to reduce the final particle size, but this is generally limited to ~1 micron and may introduce impurities from grinding media, limiting stoichiometry control. To achieve stoichiometric control for the fabrication of films, whiskers, and bulk crystals, vapor-phase reactions can be used. These were first shown for simple compounds such as SiO_2 and TiO_2. Physical vapor deposition (PVD) and chemical vapor deposition (CVD) can be used to fine tune the purity for more complex oxides but is not necessarily a scalable method (e.g., kg-size batches are not typically feasible). Additionally, this process is limited for laboratories due to costly equipment and control needed over deposition parameters.

For the synthesis of nanoparticles, liquid phase synthesis methods are very common because they require little laboratory equipment, have high stoichiometry control, and produce controlled particle size for various structures from simple fluorite structures to complex spinels. In the case of metal oxides, these techniques allow for the mixing of multiple oxides controlled on the molecular level. Hydrolysis is used to prepare simple oxides by hydrolysis of metal-organic compounds of aqueous solution of metal salts. Solvothermal is another common technique to produce high purity, fine powders performed in a solvent at a temperature between the boiling and critical point with a pressure up to the vapor pressure at the critical point [3–6]. Gel routes including sol-gel, Pechini, citrate, and glycine nitrate methods produce a semi rigid gel as an intermediate step to produce complex oxides [7]. Sol-gel uses a metal alkoxide as the oxide source, alcohol as solvent, water as hydrolysis agent, and acid or base catalyst while the other gel methods utilize common metal salts as precursors [7]. The gel methods require little laboratory equipment, making them widespread techniques for synthesis. Coprecipitation uses a solution of alkoxides or metal salts that are then precipitated using a precipitating agent. This method of synthesis creates solids with highly dispersed nanoparticles [8,9]. Additionally, this

process can synthesize compositions of elements throughout the periodic table, assuming the chemicals have similar building types, lattice types, and lattice constants on the same order of magnitude [10]. A wide variety of structures have been synthesized using this method including spinel, olivine, and wurtzite structures [10–13].

It is important to note that the list here is not exhaustive and a vast variety of synthesis techniques are used for nanoparticle synthesis. For example, in the field of drug delivery, emulsion, salting-out, nanoprecipitation, dialysis, supercritical fluid technology, solvent evaporation, and coacervation methods are used [14]. Drug delivery is a main application of nanoparticle synthesis because the uptake of nanoparticles into the body depends primarily on the size and surface characteristics of the particles.

When faced with the complexity of synthesizing complex oxide nanoparticles from scratch, you may wonder how to start the process of selecting starting materials. In the coprecipitation method where many different types of precursors can be used, it is important to choose ones that are compatible with the process. Nitrates, chlorides, acetates, sulfate, oxalates, and phosphates are among the common precursors used. Most of these are soluble in water allowing for the easy dissociation of the cation and anion for atomic mixing of the cations. One important aspect of the precursors is that they generally have structural water within the chemical. The amount of water can vary, especially for the transition metals due to multiple oxidation states. Therefore, it is important to select a precursor with a known amount of water for stoichiometry control. When a precursor hydrate is chosen with an unknown amount of water, thermal gravimetric analysis (TGA) can be used to approximate the amount of water in the material. However, this is an estimation and will lead to reduced stoichiometric control.

For example, Figure 2 shows the decomposition of manganese nitrate hydrate, a common transition metal salt that is used. The nitrate decomposes to form its oxide around 300 °C and further reduces from MnO_2 to Mn_2O_3 and finally to Mn_3O_4 [15]. The mass plateau seen for both Mn_2O_3 and Mn_3O_4 can be used to calculate the nitrate hydration but leads to small discrepancies in the hydration concentration. The decomposition analysis leads to an estimated six moles of water per mole of manganese nitrate. While TGA is able to give a good approximation of the water content, small differences between the calculated and true amount will lead to altered stoichiometry.

Most elemental precursors used in coprecipitation are soluble in water, thus allowing easy solvent preparation with a non-hazardous solvent, while other precursors will be soluble in alcohols, acetone, acids, or bases. The otherwise relatively simple synthesis process can become rather complex if multiple solvents are used. Mixing of solvents can result in intermediate interactions that disrupt the atomic mixing that occurs in coprecipitation techniques.

Therefore, it is important to be able to choose a single solvent system that works for all precursors. Achieving this common solvent process can be very complicated especially in multicomponent oxides such as high entropy oxides (HEOs) which will generally have five different cations combined. Addressing this synthesis complexity is the central theme of this work: when synthesizing complex nanoparticles, where do you begin to get it right? Here we provide a practical methodology based on commonly available precursors that provides a simplified synthesis workflow. Specifically, we detail the selection of precursors and solvents in coprecipitation methods. We have compiled data to simplify the process of selecting precursor types and solvents for the process to produce a simple solution for the precipitation of complex oxides. Using this tool, we show that this selection process can be used to synthesize two different advanced ceramic compositions, a quaternary lanthanum manganite perovskite $(La_{0.8}Ca_{0.2})(Mn_{0.8}Al_{0.2})O_{3-\delta}$ used in high temperature heterogeneous catalysis and a high entropy fluorite oxide $Ce_{0.9}(Pr_{0.025}Nd_{0.025}Sm_{0.025}Gd_{0.025})O_{2-\delta}$, a fast oxygen ion conductor.
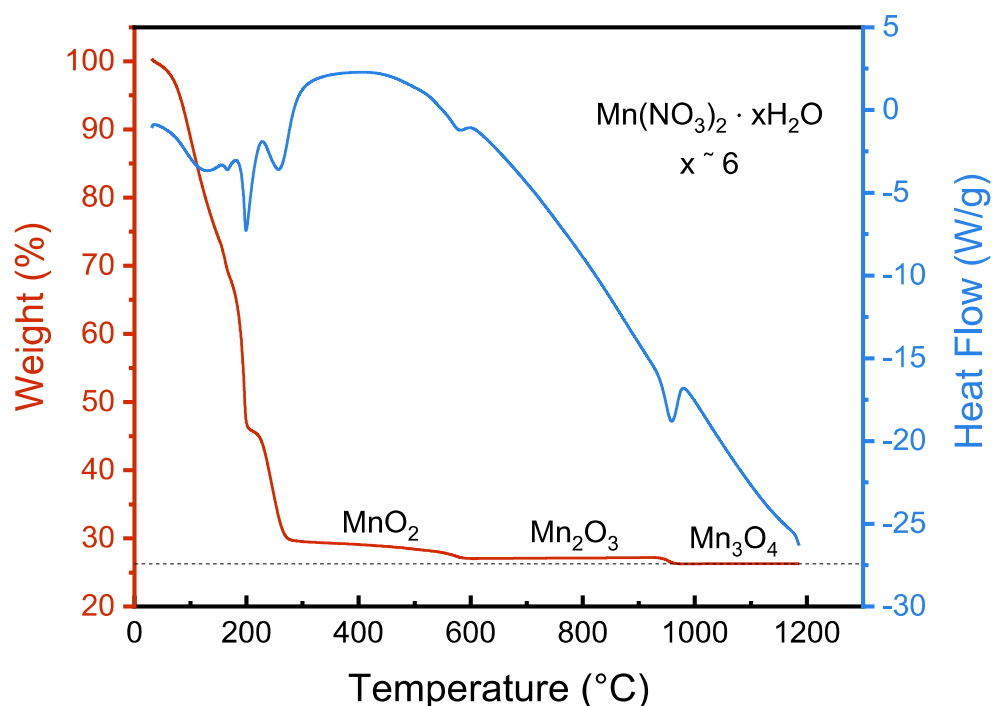
Figure 2. Simultaneous differential scanning calorimetry and thermal gravimetic analysis (SDT) of manganese nitrate hydrate performed in air from 25 to 1200 °C. The nitrate decomposes into manganese oxide and the concentration of hydrates in the crystal is approximated. The dashed line represents the theoretical weight percent of Mn_3O_4 assuming the starting precursor is $Mn(NO_3)_2 \bullet 6H_2O$.

2. Materials and Methods

2.1. Precursor Data Collection Methods

This practical methodology assembles essential information about precursors throughout the entire periodic table into two simple reference diagrams To create these reference diagrams, online searches were performed to determine commercial availability, known water in the crystal structures, melting points, and solubility of every metal salt precursor (with the salts including nitrates, chlorides, oxalates, acetates, sulfates, and phosphates). Commercial databases searched include Thermo Fisher Scientific's Fisher Scientific, Merck's MilliporeSigma, and Avantor's VWR. To compile a more inclusive list of precursor metal salts, a literature search was conducted using Clarivate's Web of Science Group database [16–30]. Searches included the name of the metal element and the salt compound, such as "lithium nitrate," for every element and salt. Phosphate precursors were excluded from reference diagrams due to their lack of availability. Sulfate precursors are shown in Figure S1 as an alternative to the four main precursors (nitrates, chlorides, acetates, and oxalates).

2.2. Experimental Methods

The two oxide compositions were synthesized using oxalate coprecipitation method and solvent deficient method. The step-by-step process for both methods is presented in Figure 3.
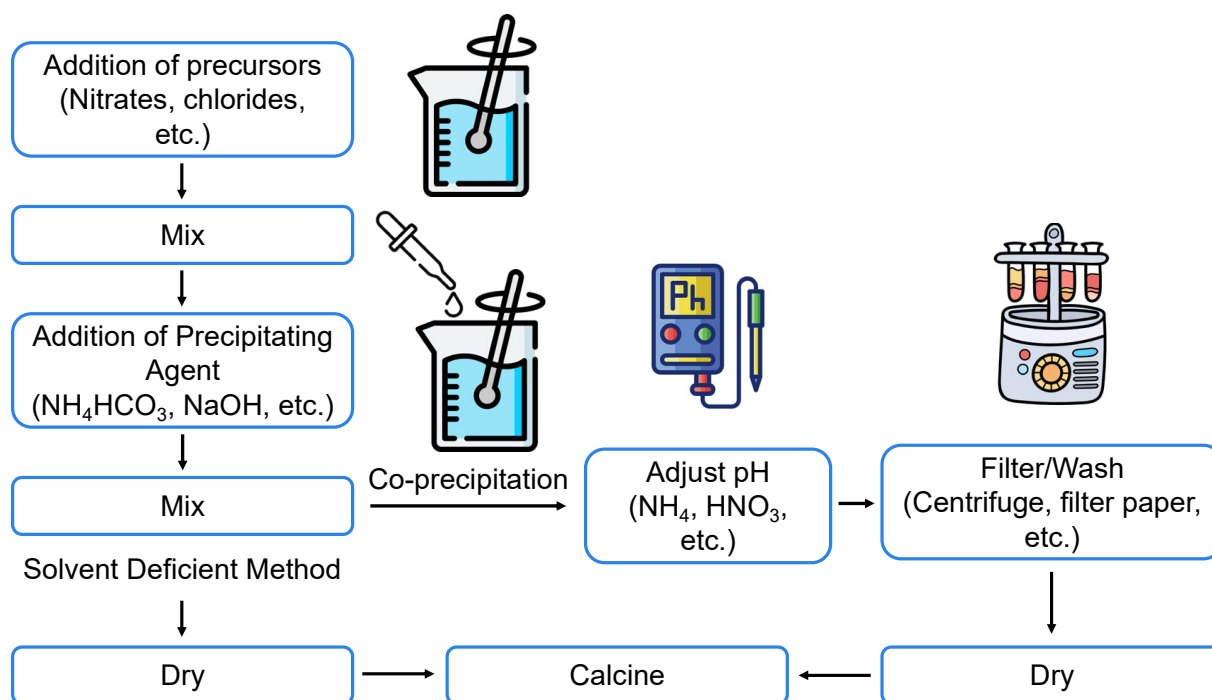
Figure 3. Flow chart of ceramic nanoparticle synthesis using co-precipitation and solvent deficient method. [Icons to illustrate the steps were created by Freepik from Flaticon.com].

2.2.1. Doped Cerium Oxide $Ce_{0.9}(Pr_{0.025}Nd_{0.025}Sm_{0.025}Gd_{0.025})O_{2-\delta}$

Doped cerium oxide was synthesized using the oxalate method. Cerium nitrate hexahydrate (99.99%), gadolinium nitrate hexahydrate (99.9%), neodymium nitrate hexahydrate (99.9%), praseodymium nitrate hexahydrate (99.9%), and samarium nitrate hexahydrate (99.999%) were used as precursors and anhydrous oxalic acid was used as the precipitating agent. Stoichiometric amounts of the nitrates were first dissolved in water in a 1M concentration. In a separate beaker, oxalic acid was dissolved in water in a 0.1 M concentration. The solutions were mixed individually for approximately 10 min. Then, the nitrate solution was added dropwise to the oxalic acid solution under vigorous stirring. Precipitation was immediate. After the entire solution was added, the sample was aged for approximately 15 min. The sample was then centrifuged and washed twice with deionized water to separate the precipitate. The sample was dried overnight at 80 °C before being ground and calcined at 900 °C for 4 h.

2.2.2. Doped Lanthanum Manganite $(La_{0.8}Ca_{0.2})(Mn_{0.8}Al_{0.2})O_{3-\delta}$ (LCMA)

Doped lanthanum manganite was synthesized using the solvent deficient method introduced by Smith et al. [31]. Metal nitrates of lanthanum, calcium, manganese, and aluminum were used as precursors. Ammonium bicarbonate was added to the measured nitrates in a 1:1 molar ratio of NH_4HCO_3 to NO_3^-. Additional water was added as solvent to increase the moles of water to 9 per mole of cation from the nitrates. The materials were then mixed using a mortar and pestle for approximately 20 min until bubbling from CO_2 release stopped. The mixture was then dried in an oven at 80 °C overnight and calcined at 600 °C for 2 h.

2.3. Characterization Methods

X-ray diffraction (XRD) patterns were collected from the oxalate precursor of the doped cerium oxide, the calcined doped cerium oxide, and the doped lanthanum manganite using a diffractometer (Panalytical XPert Powder). Diffraction was performed using a Cu X-ray source with a voltage of 45 kV, step size of 0.0167°, dwell time of 10 s, and current of 40 mA. GSAS–II was used to fit and refine the XRD patterns.

Scanning electron microscopy (SEM) and energy dispersive spectroscopy (EDS) was performed on the calcined powders using a Tescan Mira3 SEM and an EDAX Octane Pro. An accelerating voltage of 10 kV was used for the LCMA sample while 12 kV was used for the ceria high entropy oxide. A working distance of 15 mm was used for both samples. SEM and EDS performed on the doped cerium oxalate powders was performed using a Phenom XL G2 Desktop SEM.

3. Results and Discussion

3.1. Precursor Selection Tools

To successfully synthesize complex multicomponent oxides, the properties of the precursor and solvent materials must first be analyzed to determine the optimal starting materials.

3.1.1. Availability of Metal Salts

When selecting precursors for synthesis, it is important to attempt to select precursors within the same family (i.e., all nitrates or all chlorides) to limit the number of intermediate reactions that may occur. The availability of nitrates, chlorides, oxalates, and acetates are shown in Figure 4. Compiled data for sulfates is shown in the supplementary information. For elements with atomic number below 87, metal salts are commercially available. With the exception of Th, elements with atomic number above 87, are not commercially available as metal salts. Additionally, the noble gases, halogens, and other gases are understandably not available, although in the case of some halogens, they are often part of the metal salt composition. Chlorides are the most widely available metal salt followed by nitrates, acetates, and oxalates, respectively. The wide availability of metal salts opens possibilities to make complex oxides with a variety of elemental compositions.

3.1.2. Melting/Decomposition Temperature

Prior to synthesis batching, precursors are often dried to remove any absorbed water that occurred during storage. Metal salts are hygroscopic materials and are generally stored in desiccators. However, even in a desiccator, the material may absorb water, thus altering the chemical formula of the material. A change in the water content that is not accounted for will alter the stoichiometry of the material. Therefore, it is desirable to dry the material prior to weighing to remove excess water. Before drying the material, the melting temperature and/or decomposition temperature of the material should be known to ensure the material is not being altered during drying. The known melting or decomposition temperature (whichever is lower) for the metal salts is displayed in Figure 4. A temperature greater than 100 °C is desired for drying. Materials between 30 °C and 100 °C cannot be dried due to risk of altering the material. For handling purposes, materials with a melting temperature below 30 °C are also listed. These present additional challenges during weighing since they melt at room temperature and are generally stored in refrigerators.

3.1.3. Hydration

When selecting metal salts to use in synthesis, it is important to know the chemical formula of the chemical selected. Metal salts often contain structural water that can vary depending on the crystal structure that forms. Some metal salts can form in multiple structures with a variable number of water molecules, thus making their water concentration vary from batch to batch. These metal salts are denoted as hydrate rather than a specified concentration of waters and that variability must be considered when batching for synthesis. If the selected precursor does not have a designated concentration of hydrates, the stoichiometry of the mixture may be off. Figure 4 shows the compiled commercial data for the hydration of nitrates, chlorides, acetates, and oxalates. As shown, most metal salts that are commercially available can be acquired with a known amount of water. However, the metal salts in red are only available as hydrates. This presents a challenge when batching for synthesis. Additionally, while some metal salts may be available with a known water content, the hydrate may be available at a higher purity. For example, manganese nitrate

tetrahydrate, while available at a tetrahydrate, is only available up to 98% purity whereas manganese nitrate hydrate is available at 99.995% purity. Furthermore, the price for hydrate metal salt precursors is significantly lower than for a known hydrate. Therefore, while a known hydrate may be available, there may be instances where an unknown hydrate is selected instead. While the hydration can be estimated, as shown in Figure 2, this may lead to changes in the stoichiometry of the synthesized material. Therefore, if stoichiometry control is needed within a material, precursors with known hydration should be chosen.
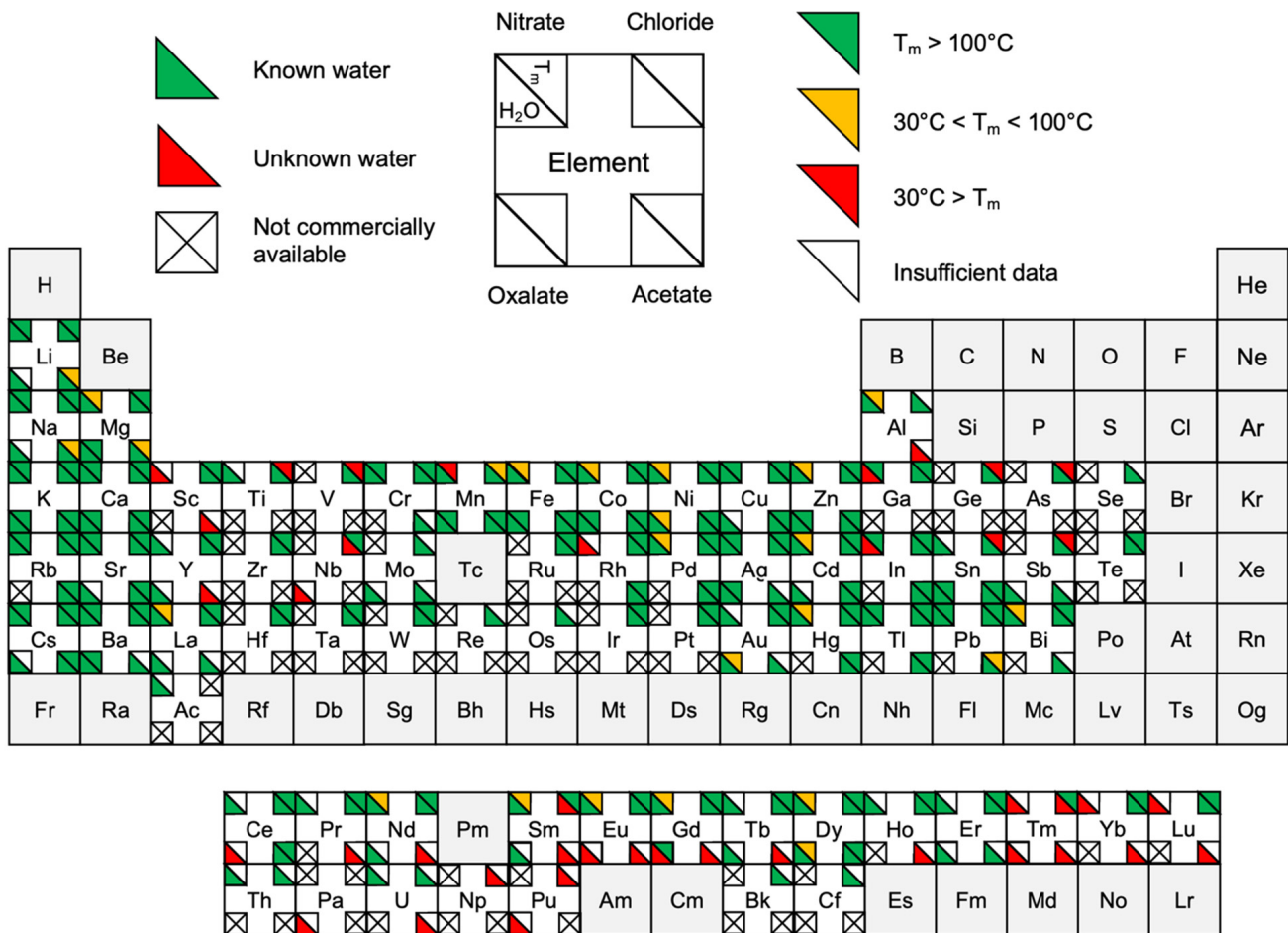
Figure 4. Periodic table of elements detailing the hydration concentration and melting temperature for commercially available precursors. The four corners in each element contain precursor information for nitrates, chlorides, oxalates, and acetates as designated in the key. Grey shaded elements with no information did not show any available commercial precursors for the four types identified. A square with an "x" shows that that specific precursor is not commercially available. The bottom left triangle in a corner informs whether the precursor contains known moles of water in the crystal lattice where green shows that the chemical can be purchased with a known hydration concentration and red shows that the chemical can only be purchased with an unknown hydration concentration. The top right triangle of a corner depicts the range containing the precursor's melting temperature: green for a melting temperature greater than 100 °C, yellow for between 30 °C and 100 °C, red for below 30 °C, and white for insufficient data to determine the melting temperature.

3.1.4. Solvent Selection

After the precursors have been selected, the next step in the process is to select the solvent. The solvent that should be used is dependent on the precursors to ensure that they can be properly dissolved. Figure 5 displays the solubility of the metal salts. When synthesizing materials, it is often desired to use water as the solvent to limit hazardous waste. When the precursors have low solubility in water, the pH can also be altered to increase the solubility of the substances. This can be done by altering to acidic conditions with acids such as nitric or hydrochloric acid or to basic conditions with bases such as ammonium or sodium hydroxide. Alcohols may be used as an alternative to water when precursors are insoluble to water. When selecting a solvent, it is desired to only use one solvent to minimize side reactions and maintain full solubility. Therefore, it is important to consider both the precursor types and solvents during the selection process to choose systems that are compatible. If a fully compatible solvent is not able to be used, an alternative precursor type should be used, or a different synthesis method may need to be used. In the case of the commercially available nitrates, all are soluble in water. Therefore, if the selected precursors are all nitrates, it is likely that water is the easiest solvent to use. When not all selected precursors are soluble in water but one or more are soluble in acid, low pH will be the preferable solvent since if things are soluble in water, they are likely soluble in acid. Additionally, when selecting a solvent, it is important to consider the settling rate of the precipitated material. In the synthesis of complex, multi-component oxides, different elemental precipitates will have different settling rates which can cause segregation of the precipitated material. To minimize differences in settling, the pH of the system can be varied. The precipitating agent can also be altered to minimize the difference in settling rate, and where possible, methods like the solvent deficient method that reduce the solvent amount can be used. Other methods that are able to form a single phase precipitate, like the oxalate method in the case of rare-earth elements, will not segregate upon sedimentation.

3.2. Test Cases

To demonstrate the effectiveness of the method outlined above, two multicomponent oxides were synthesized and characterized.

3.2.1. Fluorites

High entropy oxides utilize 4 to 5 dopants of equimolar concentration to form a single phase material. The high configurational entropy resulting from the number of elements in the material dominates over the enthalpy of unfavorable secondary phases. High entropy materials, first shown for alloys, have been extended to oxides in recent years. Different rock salt, fluorite, pyrochlore, spinel, bixbyite, and perovskite structures have all been successfully synthesized using 4 or more elements [32,33]. The large number of different structures that can be used for high entropy oxides opens the door to further innovation through controlled synthesis for tunable properties. Utilizing the tools described above to determine precursors and solvents, complex oxides can be synthesized using coprecipitation. To show the use of these tools we have synthesized the high entropy fluorite oxide, $Ce_{0.9}(Pr_{0.025}Nd_{0.025}Sm_{0.025}Gd_{0.025})O_{2-\delta}$, using the oxalate method that starts with nitrates to produce oxalates.
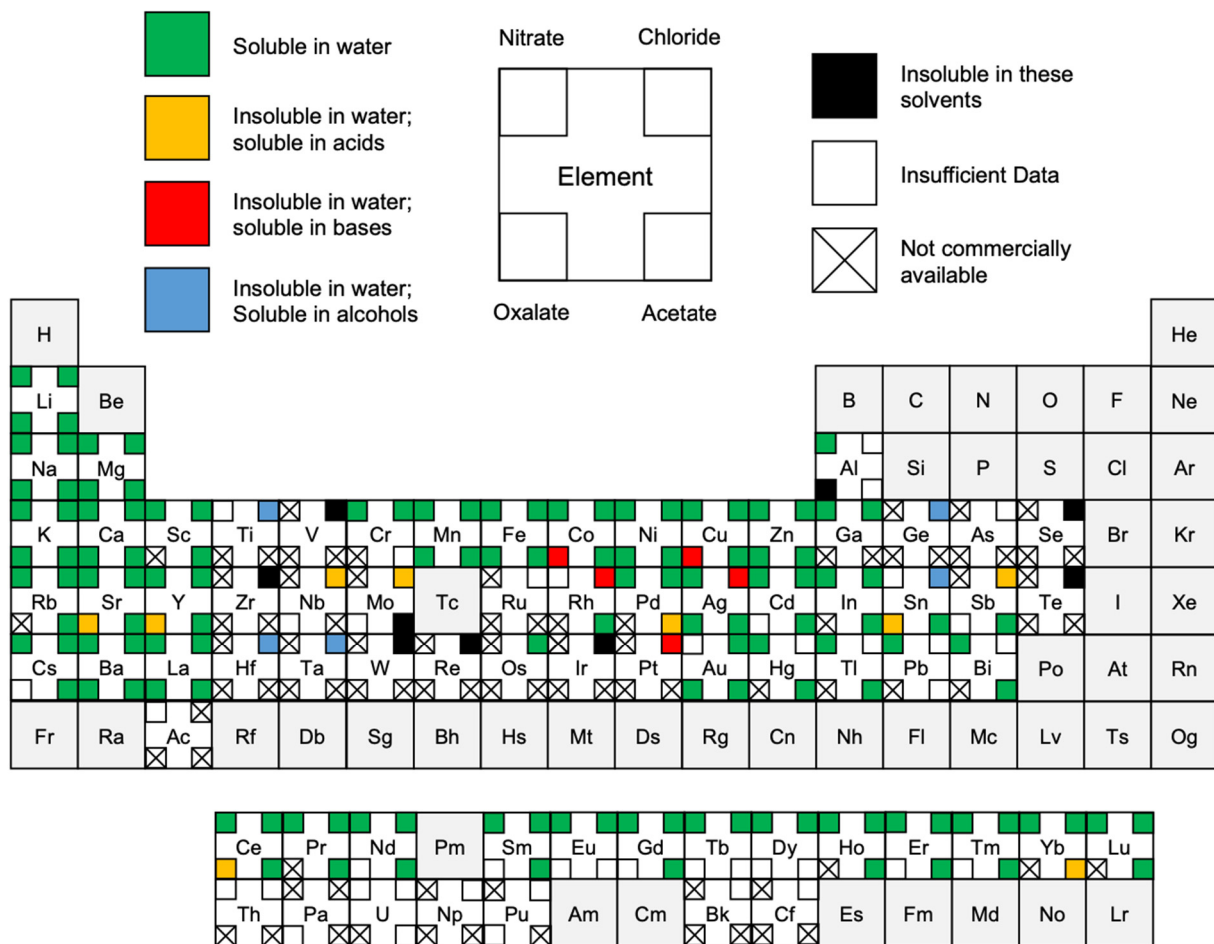
Figure 5. Periodic table of elements with solubility for available precursors. The four corners in each element contain precursor information for nitrates, chlorides, oxalates, and acetates. Greyed elements do not contain any commercially available precursors or the four investigated. A square with an "x" shows that that specific precursor is not available. The color of the square in each precursor's corner depicts its solubility, be it in water (green), acids (yellow), bases (red), alcohols (blue), or none of these solvents (black). Insufficient solubility data is shown as white.

Doped cerium oxide was synthesized starting with nitrates to produce a single phase precipitated oxalate prior to calcination. Cerium, gadolinium, neodymium, praseodymium, and samarium are all commercially available as nitrate hexahydrates. As chlorides, samarium is not available with a known hydration, thus chlorides are less desirable to use than nitrates in this situation. Additionally, for acetates and oxalates, multiple precursors are either not available or have unknown water concentrations for each group. Therefore, nitrates present the best choice for synthesis to achieve controlled stoichiometry. All the metal nitrates selected are soluble in water, allowing a simple solvent to be chosen. Using a single solvent to dissolve all the precursors at once reduces the risk of forming intermediate phases and inhomogeneous mixing.

After dissolving the nitrates in water, they were added to a mixture of dissolved oxalic acid in water to precipitate oxalates. The five elements selected (Ce, Pr, Nd, Sm, and Gd) belong to the lanthanide group and all oxalates form in the same structure as decahydrates with space group P2$_1$/c [34,35]. Alemayehu et al. recently showed that a cerium-gadolinium oxalate could be formed to produce a single phase, homogeneous oxalate [36]. Using this method with multiple cations allows for a single phase to be precipitated with mixing on the atomic scale that is improved compared to other coprecipitation methods using hydroxides or carbonates. Figure 6a displays the XRD pattern of the

precipitated oxalate after drying at 80 °C overnight. As shown, all peaks correspond to a single decahydrate oxalate in the $P2_1/c$ space group, confirming the atomic mixing that occurs during oxalate coprecipitation for the lanthanides. The powder after calcination is shown in Figure 6b with all peaks corresponding to the fluorite structure with space group Fm-3m. No secondary phases are identified in the structure. The observed XRD pattern was fit against $Ce_{0.9}Gd_{0.1}O_{2-\delta}$ (JCPDS # 01-075-0161) using GSAS-II software with a final wR = 9.49%. The lattice constant for the Ce HEO was determined to be 5.4196 Å. This is a slight increase compared to the 5.4180 Å value for $Ce_{0.9}Gd_{0.1}O_{2-\delta}$. Using multiple dopants that regularly do not form in the same structure presents challenges for synthesizing a single phase material. By utilizing a straightforward approach to selecting precursors and solvents and choosing an appropriate coprecipitation synthesis technique, multicomponent oxides can be synthesized with high purity and high stoichiometry control.

EDS was performed on the oxalate precursor and calcined ceria HEO to confirm uniformity within the material. Figure 7 shows the EDS data acquired for individual particles of the oxalate precursor and calcined material. Each element shows homogenous distribution in the particle with no rich or depleted regions shown. Due to the overlapping K shell energies and low counts for the L shell arising from low concentration levels, attempts to do an actual stoichiometric calculation are not feasible. The low concentration of each element produces large error in the EDS calculation. However, the total calculated dopant concentration was found to be 10%, matching the desired amount and confirming the synthesis process. The EDS confirms the approximate stoichiometry of the material, the even distribution of elements in the material, and the single phase XRD that was acquired.

3.2.2. Perovskites

Perovskites are widely used materials that are of great interest due to their high degree of tunability from the numerous doping elements available. The ABO_3 structure offers two sites for doping, the a and b sites, and can accommodate significant lattice distortions. Elements with varying oxidation states have been used to dope these materials, encompassing most of the periodic table. With the large number of elements possible to alter the structure, perovskites are a perfect test case to choose from the wide number of metal salts available.

$(La_{0.8}Ca_{0.2})(Mn_{0.8}Al_{0.2})O_{3-\delta}$ (LCMA) was synthesized using the solvent deficient method. This method was selected as an alternative to other coprecipitation methods because it does not require a filtering step. In the well-studied case of manganese nickel spinel, there is difficulty producing the desired stoichiometry due to differences in precipitant solubilities [37]. Additionally, in the case of the synthesis of $(La_{0.8}Sr_{0.2})(Ga_{0.8}Mg_{0.2})O_{3-\delta}$ using coprecipitation, Pelosato et al. showed that when using NH_4OH and $(NH_4)_2CO_3$ as precipitation agents, the total strontium loss can be greater than 50% [38]. Therefore, by utilizing SDM, loss of precursor in the mother liquor will not occur, allowing better control over stoichiometry.

Mullen et al. synthesized LSMA nanoparticles using a microwave-assisted hydrothermal method but used $Mn(NO_3)_2 \cdot xH_2O$ rather than manganese nitrate tetrahydrate [39]. The x value was approximated to be 4 which may have led to overestimation of the manganese concentration in the final product, leading to an excess of aluminum in the material. While it is not stated in the manuscript, there is a secondary peak seen at approximately 30°, which is likely an aluminum rich phase that occurred due to off-stoichiometry from approximating the x value of manganese nitrate. Therefore, only nitrates with known water concentrations were chosen for the synthesis of LCMA.

(a)

(b)
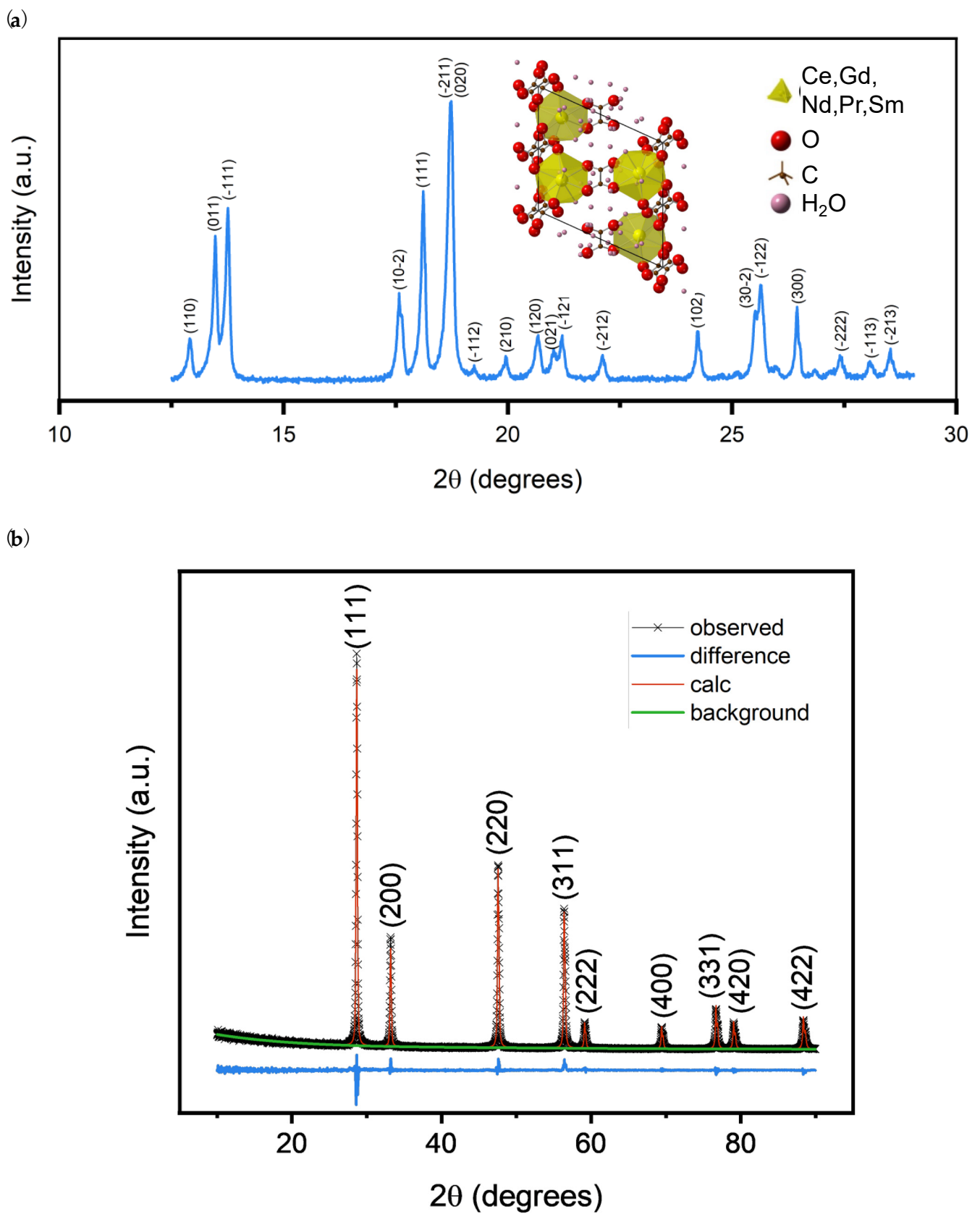
Figure 6. XRD patterns of the (**a**) oxalate precursor and (**b**) calcined Ce HEO. The calcined Ce HEO pattern (crosses) was refined using GSAS–II software to show single phase purity.
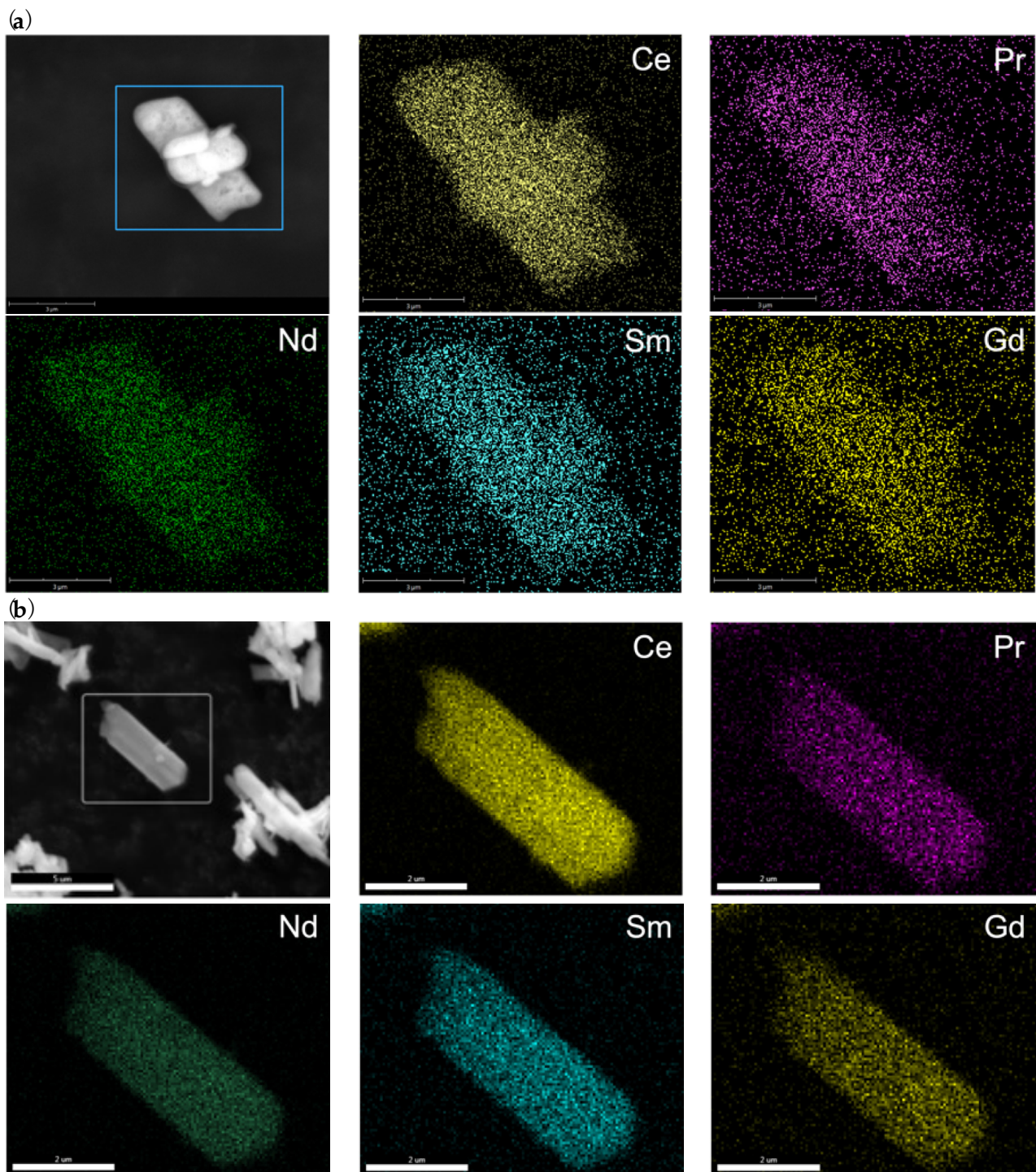
Figure 7. EDS data for (**a**) oxalate precursor and (**b**) calcined Ce HEO displaying homogeneous distribution of cations.

After fully reacting with the ammonium bicarbonate, LCMA was calcined at 600 °C for 2 h. The calcination temperature was selected based on decomposition data recorded from simultaneous differential scanning calorimeter and thermal gravimetric analyzer. As shown in Figure 8, the material forms in the perovskite phase with no observance of secondary phases. The broadening of the peaks is the result of small crystallite size, which was estimated using the well-known Scherrer's equation to be 14 nm, assuming a K value of 0.94. Although the value of K varies based on the shape, the value of 0.94 used here to approximate the crystallite size, assuming spherical and homogeneous shape.
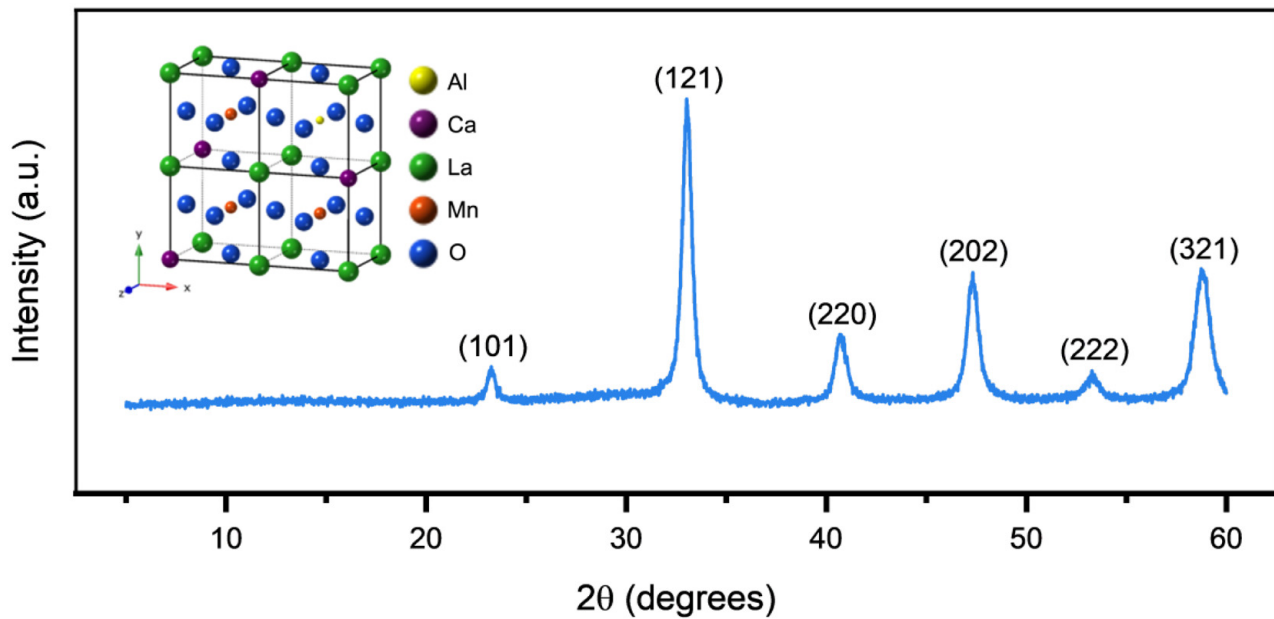
Figure 8. XRD pattern of the calcined LCMA powder displaying phase pure powder in the perovskite structure.

Figure 9 displays the EDS data for the LCMA powder. As seen, the elements are homogeneously distributed in the powder, confirming phase uniformity and single phase synthesis of LCMA. By using precursors with known stoichiometry, LCMA was successfully synthesized as a homogeneous material even after thermal treatment. Overall, these two examples showcase the practical implementation of the methodology presented here to synthesize high purity, complex materials successfully.
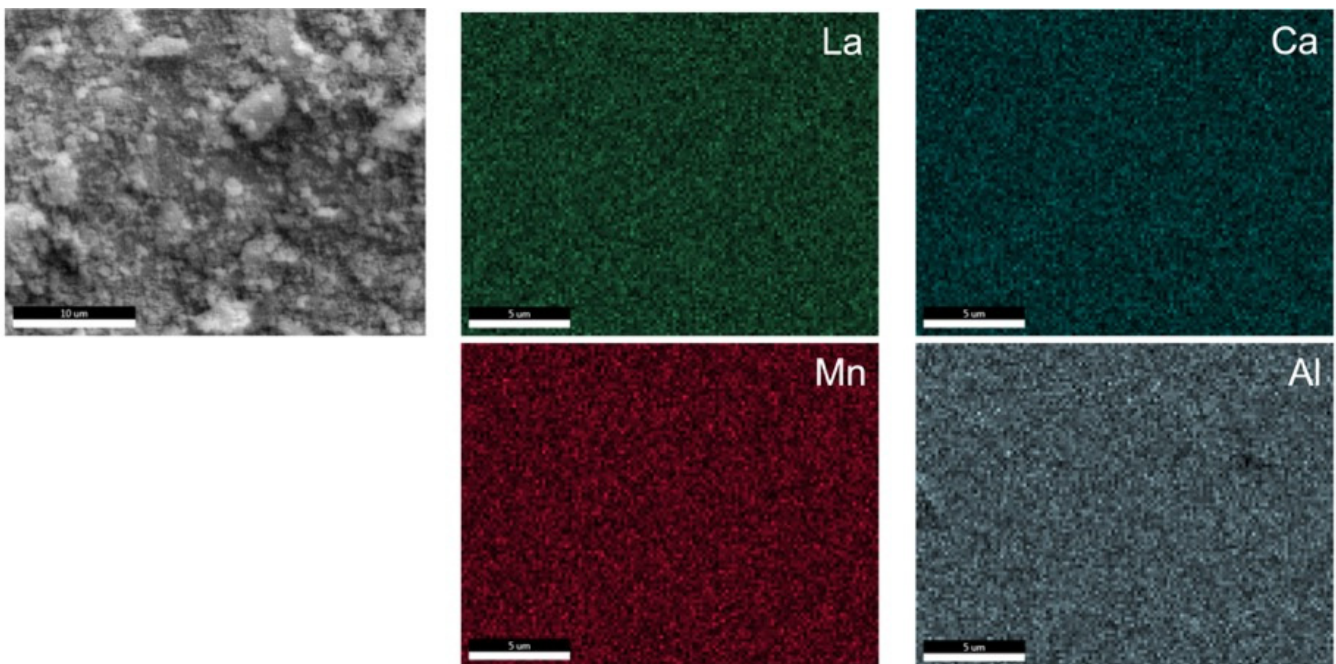
Figure 9. SEM and EDS mapping for La, Ca, Mn, and Al of the LCMA powder showing homogeneous distribution.

4. Conclusions

The synthesis of high purity, stoichiometric nanoparticles, requires control from the beginning of the batching process with selection of precursors. To properly select precursors, the hydration, melting temperature, and solubility need to be identified prior to use. We showed a methodology where by identifying the precursor family with known hydration concentration, complex ceramics with multication concentrations can be successfully synthesized as single phase with homogeneous cation distribution. The high entropy oxide, $Ce_{0.9}(Pr_{0.025}Nd_{0.025}Sm_{0.025}Gd_{0.025})O_{2-\delta}$ was synthesized using the oxalate method. This method started with all five elements as metal nitrates with known hydration. This allowed for correct batching of the elements and the phase purity was confirmed by XRD and EDS. A co-doped perovskite, $(La_{0.8}Ca_{0.2})(Mn_{0.8}Al_{0.2})O_{3-\delta}$ was also synthesized using a solvent deficient method beginning with nitrates of known hydration. XRD and EDS of the material showed that single phase purity of the material is able to be successfully synthesized using this method.

References

1. Gnesin, G.G. Revisiting the History of Materials Science on the Origin and Development of Ceramic Technology. *Powder Metall. Met. Ceram.* **2012**, *51*, 496–501. [CrossRef]
2. Advanced Ceramics—Timeline. Science Learning Hub. Available online: https://www.sciencelearn.org.nz/resources/1793-advanced-ceramics-timeline (accessed on 20 June 2022).
3. Yu, S.-H. Hydrothermal/Solvothermal Processing of Advanced Ceramic Materials. *J. Ceram. Soc. Japn.* **2001**, *109*, S65–S75. [CrossRef]
4. Choi, H.G.; Jung, Y.H.; Kim, D.K. Solvothermal Synthesis of Tungsten Oxide Nanorod/Nanowire/Nanosheet. *J. Am. Ceram. Soc.* **2005**, *88*, 1684–1686. [CrossRef]
5. Spiridigliozzi, L.; Ferone, C.; Cioffi, R.; Accardo, G.; Frattini, D.; Dell'Agli, G. Entropy-Stabilized Oxides Owning Fluorite Structure Obtained by Hydrothermal Treatment. *Materials* **2020**, *13*, 558. [CrossRef]
6. Byrappa, K. Novel Hydrothermal Solution Routes of Advanced High Melting Nanomaterials Processing. *J. Ceram. Soc. Japn.* **2009**, *117*, 236–244. [CrossRef]
7. Chilibon, I.; Marat-Mendes, J.N. Ferroelectric Ceramics by Sol–Gel Methods and Applications: A Review. *J. Sol.-Gel. Sci. Technol.* **2012**, *64*, 571–611. [CrossRef]
8. Huang, Z.; Han, W.; Feng, Z.; Qi, J.; Wu, D.; Wei, N.; Tang, Z.; Zhang, Y.; Duan, J.; Lu, T. The Effects of Precipitants on Co-Precipitation Synthesis of Yttria-Stabilized Zirconia Nanocrystalline Powders. *J. Sol.-Gel. Sci. Technol.* **2019**, *90*, 359–368. [CrossRef]
9. Colomban, P. Chemical Preparation Routes and Lowering the Sintering Temperature of Ceramics. *Ceramics* **2020**, *3*, 312–339. [CrossRef]

10. Kolthoff, I.M. Theory of Coprecipitation. The Formation and Properties of Crystalline Precipitates. *J. Phys. Chem.* **1932**, *36*, 860–881. [CrossRef]

11. Sinkó, K.; Szabó, G.; Zrínyi, M. Liquid-Phase Synthesis of Cobalt Oxide Nanoparticles. *J. Nanosci. Nanotech.* **2011**, *11*, 4127–4135. [CrossRef]

12. Tavakoli, H.; Sarraf-Mamoory, R.; Zarei, A. Inverse Co-Precipitation Synthesis of Copper Chromite Nanoparticles. *Iran. J. Chem. Chem. Eng.-Int. Engl. Ed.* **2016**, *35*, 51–55.

13. Dong, H.; Koenig, G. A Review on Synthesis and Engineering of Crystal Precursors Produced Via Coprecipitation for Multicomponent Lithium-Ion Battery Cathode Materials. *CrystEngComm* **2019**, *22*, 1514–1530. [CrossRef]

14. Merlin, J.J.; Rajan, S.S. A Review on Synthesis and Preparation of Nanoparticles. *J. Cancer Sci. Treat.* **2020**, *2*, 87–89.

15. Jian, G.; Xu, Y.; Lai, L.-C.; Wang, C.R.; Zachariah, M. Mn3O4 Hollow Spheres for Lithium-Ion Batteries with High Rate and Capacity. *J. Mater. Chem. A* **2014**, *2*, 4627–4632. [CrossRef]

16. Dale, G.E.; Dalmas, D.A.; Gallegos, M.J.; Jackman, K.R.; Kelsey, C.T.I.; May, I.; Reilly, S.D.; Stange, G.M. 99Mo Separation from High-Concentration Irradiated Uranium Nitrate and Uranium Sulfate Solutions. *Ind. Eng. Chem. Res.* **2012**, *51*, 13319–13322. [CrossRef]

17. Andersson, S.; Nitsche, H.; Sudowe, R. Berkelium Nitrate Complex Formation Using a Solvent Extraction Technique. *Radiochim. Acta* **2006**, *94*, 59–61. [CrossRef]

18. Smith, R.C.; Hoilien, N.; Dykstra, C.; Campbell, S.A.; Roberts, J.T.; Gladfelter, W.L. Chemical Vapor Deposition of TixSi1–XO2 Films: Precursor Chemistry Impacts Films Composition. *Chem. Vap. Depos.* **2003**, *9*, 79–86. [CrossRef]

19. Kim, D.-H.; Park, T.-H.; Bae, S.-E.; Lee, N.; Kim, J.-Y.; Cho, Y.-H.; Yeon, J.-W.; Song, K. Electrochemical Preparation and Spectroelectrochemical Study of Neptunium Chloride Complexes in LiCl–KCl Eutectic Melts. *J. Radioanal. Nucl. Chem.* **2016**, *308*, 31–36. [CrossRef]

20. Homma-Takeda, S.; Terada, Y.; Nakata, A.; Sahoo, S.K.; Yoshida, S.; Ueno, S.; Inoue, M.; Iso, H.; Ishikawa, T.; Konishi, T.; et al. Elemental Imaging of Kidneys of Adult Rats Exposed to Uranium Acetate. *Nucl. Instrum. Methods Phys. Res. Sect. B Beam Interact. Mater. Atoms* **2009**, *267*, 2167–2170. [CrossRef]

21. Galley, S.S.; Gaggioli, C.A.; Zeller, M.; Celis-Barros, C.; Albrecht-Schmitt, T.E.; Gagliardi, L.; Bart, S.C. Evidence of Alpha Radiolysis in the Formation of a Californium Nitrate Complex. *Chem. Eur. J.* **2020**, *26*, 8885–8888. [CrossRef]

22. Murali, A.; Sohn, H.Y. Plasma-Assisted Chemical Vapor Synthesis of Indium Tin Oxide (ITO) Nanopowder and Hydrogen-Sensing Property of ITO Thin Film. *Mater. Res. Express* **2018**, *5*, 065045. [CrossRef]

23. Abrão, A.; de Freitas, A.A.; de Carvalho, F.M.S. Preparation of Highly Pure Thorium Nitrate via Thorium Sulfate and Thorium Peroxide. *J. Alloys Compd.* **2001**, *323–324*, 53–56. [CrossRef]

24. Yoshihara, K.; Kanno, M.; Mukaibo, T. Preparation of Uranium Disulfide from Uranium Chloride. *J. Nucl. Sci. Technol.* **1967**, *4*, 578–581. [CrossRef]

25. Stroud, M.; Salazar, R.; Sandoval, A.; Garcia, V.; Danis, J.; Abney, K.; Hatler, V. Purification of Aqueous Plutonium Chloride Solutions via Precipitation and Washing. In *Abstracts of Paper of the American Chemical Society*; American Chemical Society: Washington, DC, USA, 2003; Volume 226, p. U633.

26. Wenzel, A.W.; Pietri, C.E. Purification of Plutonium Sulfate Tetrahydrate by Recrystallization and Ion Exchange. *Anal. Chem.* **1963**, *35*, 1324–1325. [CrossRef]

27. Corbey, J.; Sweet, L.; Sinkov, S.; Reilly, D.; Parker, C.; Lonergan, J.; Johnson, T. Quantitative Microstructural Characterization of Plutonium Oxalate Auto-Degradation and Evidence for PuO2 Nanocrystal Formation. *Eur. J. Inorg. Chem.* **2021**, *2021*, 3277–3291. [CrossRef]

28. Young, J.P.; Shaw, R.W.; Webb, O.F. Radioactive Origin of Emissions Observed from Uranium Compounds and Their Silica Cells. *Inorg. Chem.* **1999**, *38*, 5192–5194. [CrossRef]

29. Muxart, R.; Vernois, J.; Guillaum, R.; Arapakis, H. Studies on Protactinium Oxalate. *Bull. Soc. Chim. Fr.* **1967**, *8*, 2890.

30. Kremer, C.B. The Purification of Thorium Chloride Octahydrate. *J. Am. Chem. Soc.* **1942**, *64*, 1009–1010. [CrossRef]

31. Smith, S.J.; Huang, B.; Liu, S.; Liu, Q.; Olsen, R.E.; Boerio-Goates, J.; Woodfield, B.F. Synthesis of Metal Oxide Nanoparticles via a Robust "Solvent-Deficient" Method. *Nanoscale* **2015**, *7*, 144–156. [CrossRef]

32. Akrami, S.; Edalati, P.; Fuji, M.; Edalati, K. High-Entropy Ceramics: Review of Principles, Production and Applications. *Mater. Sci. Eng. R Rep.* **2021**, *146*, 100644. [CrossRef]

33. Tseng, K.-P.; Yang, Q.; McCormack, S.J.; Kriven, W.M. High-Entropy, Phase-Constrained, Lanthanide Sesquioxide. *J. Am. Ceram. Soc.* **2020**, *103*, 569–576. [CrossRef]

34. Alemayehu, A.; Zakharanka, A.; Tyrpekl, V. Homogeneous Precipitation of Lanthanide Oxalates. *ACS Omega* **2022**, *7*, 12288–12295. [CrossRef] [PubMed]

35. Ollendorff, W.; Weigel, F. The Crystal Structure of Some Lanthanide Oxalate Decahydrates, Ln2(C2O4)3·10H2O, with Ln = La, Ce, Pr, and Nd. *Inorg. Nucl. Chem. Lett.* **1969**, *5*, 263–269. [CrossRef]

36. Alemayehu, A.; Zákutná, D.; Kohúteková, S.; Tyrpekl, V. Transition between Two Solid-Solutions: Effective and Easy Way for Fine Ce1−xGdxO2−x/2 Powders Preparation. *J. Am. Ceram. Soc.* **2022**, *105*, 4621–4631. [CrossRef]

37. Wang, D.; Belharouak, I.; Zhou, G.; Amine, K. Synthesis of Lithium and Manganese-Rich Cathode Materials via an Oxalate Co-Precipitation Method. *J. Electrochem. Soc.* **2013**, *160*, A3108. [CrossRef]

38. Pelosato, R.; Cristiani, C.; Dotelli, G.; Latorrata, S.; Ruffo, R.; Zampori, L. Co-Precipitation in Aqueous Medium of La$_{0.8}$Sr$_{0.2}$Ga$_{0.8}$Mg$_{0.2}$O$_{3-\delta}$ via Inorganic Precursors. *J. Power Sources* **2010**, *195*, 8116–8123. [CrossRef]

39. Mullen, M.R.; Spirig, J.V.; Hoy, J.; Routbort, J.L.; Singh, D.; Dutta, P.K. Development of Nanosized Lanthanum Strontium Aluminum Manganite as Electrodes for Potentiometric Oxygen Sensor. *Sens. Actuators B Chem.* **2014**, *203*, 670–676. [CrossRef]